Journal of Advanced Research 43 (2023) 45–57

Contents lists available at ScienceDirect

Journal of Advanced Research

journal homepage: www.elsevier.com/locate/jare

Original Article

TRPM1 promotes tumor progression in acral melanoma by activating the Ca^{2+}/CaMKIIδ/AKT pathway

Chi-Che Hsieh [a], Yue-Chiu Su [b], Kuan-Ying Jiang [a], Takamichi Ito [c], Ting-Wei Li [d], Yumiko Kaku-Ito [c], Shih-Tsung Cheng [b,e,f], Li-Tzong Chen [a,g,h], Daw-Yang Hwang [a], Che-Hung Shen [a,i,*]

[a] National Institute of Cancer Research, National Health Research Institutes, Tainan 704, Taiwan
[b] Department of Pathology, Kaohsiung Medical University Hospital, Kaohsiung Medical University, Kaohsiung 807, Taiwan
[c] Department of Dermatology, Graduate School of Medical Sciences, Kyushu University, Fukuoka 812-8582, Japan
[d] Department of Life Sciences, National Cheng Kung University, Tainan 704, Taiwan
[e] Department of Dermatology, Kaohsiung Medical University Hospital, Kaohsiung Medical University, Kaohsiung 807, Taiwan
[f] Department of Dermatology, College of Medicine, Kaohsiung Medical University, Kaohsiung 807, Taiwan
[g] Department of Internal Medicine, Kaohsiung Medical University Hospital, Kaohsiung Medical University, Kaohsiung 807, Taiwan
[h] Center for Cancer Research, Kaohsiung Medical University, Kaohsiung 807, Taiwan
[i] Ph.D. Program in Tissue Engineering and Regenerative Medicine, Biotechnology Center, National Chung Hsing University, Taichung 402, Taiwan

HIGHLIGHTS

- TRPM1 was associated with the progression and shorter survival in patients with acral melanoma.
- TRPM1 upregulated the Ca^{2+}/CaMKIIδ/AKT signaling to promote acral melanoma.
- The phospho-CaMKIIδ at T287 was required for the tumor-promoting activity of TRPM1 *in vitro*.
- KN93, a CaMKII inhibitor, reduced TRPM1-promoted CaMKIIδ/AKT cascade, cell growth, and mobility.
- KN93 suppressed the growth of acral melanoma cells with high TRPM1 expression *in vitro* and *in vivo*.

GRAPHICAL ABSTRACT

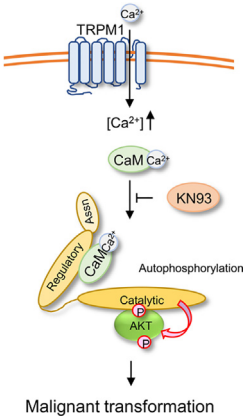

ARTICLE INFO

Article history:
Received 25 November 2021
Revised 27 February 2022
Accepted 2 March 2022
Available online 12 March 2022

Keywords:
Acral melanoma
TRPM1
CaMKII
Ca^{2+} channel

ABSTRACT

Introduction: Acral melanoma is a predominant and aggressive subtype of melanoma in non-Caucasian populations. There is a lack of genotype-driven therapies for over 50% of patients. TRPM1 (transient receptor potential melastatin 1), a nonspecific cation channel, is mainly expressed in retinal bipolar neurons and skin. Nonetheless, the function of TRPM1 in melanoma progression is poorly understood.
Objectives: We investigated the association between TRPM1 and acral melanoma progression and revealed the molecular mechanisms by which TRPM1 promotes tumor progression and malignancy.
Methods: TRPM1 expression and CaMKII phosphorylation in tumor specimens were tested by immunohistochemistry analysis and scored by two independent investigators. The functions of TRPM1 and CaMKII were assessed using loss-of-function and gain-of-function approaches and examined by western blotting, colony formation, cell migration and invasion, and xenograft tumor growth assays. The effects of a CaMKII inhibitor, KN93, were evaluated using both *in vitro* cell and *in vivo* xenograft mouse models.

Peer review under responsibility of Cairo University.
* Corresponding author at: National Institute of Cancer Research, National Health Research Institutes, No. 367, Sheng-Li Rd., North District, Tainan 70456, Taiwan.
E-mail address: chshen@nhri.edu.tw (C.-H. Shen).

https://doi.org/10.1016/j.jare.2022.03.005
2090-1232/

Results: We revealed that TRPM1 protein expression was positively associated with tumor progression and shorter survival in patients with acral melanoma. TRPM1 promoted AKT activation and the colony formation, cell mobility, and xenograft tumor growth of melanoma cells. TRPM1 elevated cytosolic Ca^{2+} levels and activated CaMKIIδ (Ca^{2+}/calmodulin-dependent protein kinase IIδ) to promote the CaMKIIδ/AKT interaction and AKT activation. The functions of TRPM1 in melanoma cells were suppressed by a CaMKII inhibitor, KN93. Significant upregulation of phospho-CaMKII levels in acral melanomas was related to increased expression of TRPM1. An acral melanoma cell line with high expression of TRPM1, CA11, was isolated from a patient to show the anti-tumor activity of KN93 *in vitro* and *in vivo*.
Conclusions: TRPM1 promotes tumor progression and malignancy in acral melanoma by activating the Ca^{2+}/CaMKIIδ/AKT pathway. CaMKII inhibition may be a potential therapeutic strategy for treating acral melanomas with high expression of TRPM1.

Introduction

Melanoma is a malignant transformation of melanocytes that most frequently starts in the skin. Acral melanoma, which originates in the glabrous skin of the palms, soles, and nail beds, is a rare subtype in Caucasian populations. However, it is the most common subtype of melanoma in Asian, African, and Latin American populations [1,2]. Acral melanoma occurs in areas of the extremities that are not frequently exposed to UV radiation and is associated with a lower mutational burden and a higher number of somatic structural aberrations. However, cutaneous melanoma occurs in areas exposed to UV radiation and is associated with a high mutation burden [3]. The MAPK pathway is commonly altered and plays a crucial role in melanoma pathogenesis [4]. In cutaneous melanomas, mutations in kinases of the MAPK pathway, including NRAS (15–20%) and BRAF (35–50%), have been identified and shown to play a critical role in malignant transformation and the development of drug resistance [5]. More than 90% of BRAF mutations are a single-base substitution from valine (V) to glutamic acid (E) at codon 600 in the activation segment of the kinase and lead to MAPK pathway hyperactivation. Thus, BRAFV600E is an oncogenic driver and therapeutic target [6,7]. In acral melanoma, mutations in *BRAF* (10–35%) have been identified, but the frequency is considerably lower than that in cutaneous melanomas [3,8–10]. Moreover, the amplification or deletion of many genes, such as *CDKN2A*, *CDK4* and *TERT*, is a common carcinogenic mutation in acral melanoma [1]. These pathogenic characterizations and genetic alterations make acral melanoma different from cutaneous melanoma.

TRPM1 encodes a member of the transient receptor potential melastatin subfamily of transient receptor potential ion channels. Its promoter region contains four microphthalmia-binding sites with an M−box element, suggesting it is expressed in pigmented cells, e.g., in the retina and skin [11,12]. *In-situ* hybridization analysis has shown that *TRPM1* is expressed in benign nevi, dysplastic nevi, and cutaneous melanomas and has revealed a negative association between *TRPM1* mRNA and melanoma aggressiveness [13–15]. However, a study has suggested that the tumor suppressive activity is mediated by a microRNA (miR-211) hosted within intron 6 of *TRPM1* mRNA. The manipulation of miR-211 altered the invasion activity of several cutaneous malignant melanoma cell lines and regulated the expression of *IGF2R, TGFBR2* and *NFAT5*. This study suggests that the inverse association between the levels of *TRPM1* mRNA and melanoma metastasis is caused by miR-211 instead of *TRPM1* mRNA [16]. Moreover, a study has also suggested that the expression of *TRPM1* mRNA is associated with the upregulation of miR-211-5p (mature sequence of miR-211), which activates the survival pathway in response to BRAF inhibitors in a cutaneous melanoma cell line, MML-1 [17]. However, the functional investigations of TRPM1 protein in regulating melanoma growth and malignant transformation have not yet been performed. Additionally, a relatively low correlation between expression levels of protein and mRNA has been reported [18–20].These suggest that a different approach is needed to validate the relationship between TRPM1 and melanoma progression.

TRPM1 is a nonspecific cation channel allowing cations, such as Ca^{2+}, to cross the membrane [21]. TRPM1 has been suggested to increase cytosolic Ca^{2+} concentrations in HEK293 cells [22]. In melanocytes, Knockdown of TRPM1 results in reduced intracellular Ca^{2+} concentrations, tyrosinase activity, and amount of intracellular melanin pigment, showing that TRPM1 is involved in Ca^{2+} homeostasis and melanogenesis [23]. Ca^{2+} flux has been associated with the motility of B16F10 mouse melanoma cells [24]. However, the mechanisms that mediate Ca^{2+} signaling during malignant transformation in melanoma have not yet been identified. Ca^{2+}/calmodulin-dependent kinase II (CaMKII) is a serine/threonine kinase. It is one of the most important Ca^{2+} signaling effectors activated by a Ca^{2+} surge, which results in the autophosphorylation of its catalytic domain [25,26]. Ca^{2+} complexes with calmodulin to bind and activate CaMKII by triggering the autophosphorylation of CaMKII at multiple sites within the activation loop to prolong kinase activity. This permits the integration of Ca^{2+} signal transduction by phosphorylating and activating a large number of substrates, including AKT [27].

In this study, we investigated the relationship between the TRPM1 protein level and the progression of acral melanoma in two cohorts: Kaohsiung Medical University Hospital (KMUH) in Taiwan and Kyushu University Hospital (KUH) in Japan. We found that high TRPM1 protein expression is associated with poor prognosis in patients with acral melanoma, identified that the Ca^{2+}/CaMKIIδ-dependent AKT signaling pathway mediates the tumor-promoting activity of TRPM1, and evaluated the inhibitory effects of a CaMKII inhibitor on the tumor growth of TRPM1-high melanoma cells. Our findings provide insight into the regulatory mechanism by which TRPM1 promotes melanoma malignancy and suggest how therapeutic benefits may be obtained by means of CaMKII inhibitors, such as KN93, in the treatment of acral melanoma featuring high TRPM1 expression.

Results

The level of TRPM1 protein is positively associated with tumor progression and poor survival in patients with acral melanoma

To reveal the tumor characteristics and clinical correlation between acral melanoma progression and TRPM1 protein expression internationally, we designed a cohort study including 44 patients from KMUH (Taiwan) and 43 patients from KUH (Japan). The demographic features of the 87 patients with acral melanoma are summarized in the supplementary dataset and supplementary

Table 1
The correlations between TRPM1 expression and clinicopathological parameters in the 87 patients with acral melanoma.

Parameter	Number of cases	TRPM1 H-score		X^2 statistic	TRPM1 H-score	Unpaired two-tailed Student's *t*-test
		<2 (Low)	≧2 (High)	*P* value	(mean ± SEM)	*P* value
Age (y)						
< 65	24	14	10	0.001	1.4 ± 0.2	0.358
≧ 65	63	37	26	0.973	1.6 ± 0.1	
Gender						
Male	41	22	19	0.787	1.6 ± 0.1	0.485
Female	46	29	17	0.375	1.5 ± 0.1	
Primary tumor site						
Foot	68	37	31	2.274	1.6 ± 0.1	0.021*
Hand	19	14	5	0.132	1.1 ± 0.2	
Breslow thickness						
< 2 mm	31	23	8	4.815	1.2 ± 0.2	0.008**
≧ 2 mm	56	28	28	0.028*	1.7 ± 0.1	
T category						
Tis	6	5	1		0.7 ± 0.4	
T1	14	11	3	7.394	1.2 ± 0.3	Tis vs. T1 = 0.326
T2	16	11	5	0.116	1.5 ± 0.2	Tis vs. T2 = 0.064
T3	18	9	9		1.8 ± 0.2	Tis vs. T3 = 0.009**
T4	33	15	18		1.7 ± 0.1	Tis vs. T4 = 0.005**
Ulceration						
Absent	41	27	14	1.672	1.3 ± 0.1	0.079
Present	46	24	22	0.196	1.7 ± 0.1	
Lymph node metastasis						
Absent	54	29	25	0.062	1.5 ± 0.1	0.836
Present	33	22	21	0.803	1.5 ± 0.1	
Distant metastasis						
Absent	53	34	19		1.3 ± 0.1	0.009**
Present	34	17	17	0.191	1.8 ± 0.1	
AJCC Stage						
0	6	5	1		0.7 ± 0.4	
I	17	12	5	7.250	1.3 ± 0.3	0 vs. I = 0.2
II	28	11	17	0.123	1.8 ± 0.1	0 vs. II = 0.004**
III	17	11	6		1.5 ± 0.2	0 vs. III = 0.091
IV	19	12	7		1.7 ± 0.2	0 vs. IV = 0.0.1*

*P < 0.05; **P < 0.01.

Table 1. Patients from KMUH and KUH were similar in terms of age and sex. Of these patients, 78.2% had a primary tumor on the foot; 58.6% had T3 and T4 stage acral melanoma, and 41.3% had AJCC (8th edition American Joint Committee on Cancer staging system) stage III and IV acral melanoma at first diagnosis. The average survival time was 39.4 ± 36.8 months. As expected, these findings showed that acral melanoma was associated with poor survival and was often diagnosed in advanced stages.

The specificity of anti-TRPM1 antibodies was validated before performing TRPM1 IHC analysis. We found that anti-TRPM1 antibodies detected endogenous TRPM1 at a size of approximately 170 kDa in a panel of four melanoma cell lysates (supplementary Fig. 1A). Two independent *TRPM1*-specific short-hairpin RNAs (shRNAs), #21 and #74, were expressed in MeWo cells to validate the specificity of the anti-TRPM1 antibodies. The results showed that both of the *TRPM1* shRNAs reduced TRPM1 expression compared to scrambled shRNA controls (supplementary Fig. 1B). Moreover, immunocytochemistry (ICC) analysis revealed that the levels of TRPM1 were reduced in these cells expressing TRPM1 shRNA#74 (supplementary Fig. 1C). An engineered vector expressing 3xFlag-tagged TRPM1 (3xF-TRPM1) was retrovirally delivered into A375 cells. 3xF-TRPM1 was detectable by either anti-Flag M2 or anti-TRPM1 antibodies only in cells stably expressing 3xF-TRPM1 (supplementary Fig. 1D). The ectopically expressed 3xF-TRPM1 was downregulated by expressing *TRPM1* shRNAs (supplementary Fig. 1E). These data show the specificity of the anti-TRPM1 antibodies and *TRPM1* shRNAs.

Representative images of TRPM1 IHC analysis from a panel of FFPE specimens of acral melanoma are shown in Fig. 1A. TRPM1 quantitative scoring (H-score range, 0–3) was performed by two independent investigators. A significant association was found between TRPM1 protein level and tumor thickness using the X^2 test (P = 0.028, Table 1). High expression levels of TRPM1 protein (H-score ≥ 2) were preferentially correlated with Breslow thickness (P = 0.008), T category (Tis vs. T3, P = 0.009; Tis vs. T4, P = 0.005), distant metastasis (P = 0.009), and AJCC stage (0 vs. II, P = 0.004; 0 vs. IV, P = 0.01), as determined by unpaired two-tailed Student's *t*-test (Fig. 1, B–E, and Table 1). The median overall survival (OS) of patients in the TRPM1-high group (H-score ≥ 2) and TRPM1-low group was 41.87 and 75.9 months, respectively. The survival difference between these two groups was not significant (log-rank P = 0.0658; supplementary Fig. 1F). This difference may be derived from the short survival of 34 patients with distant metastasis, who had a median OS of only 31.7 months. After the exclusion of patients with distant metastasis, Kaplan–Meier survival curves revealed a tendency toward significantly shorter OS of patients with TRPM1-high acral melanoma (median OS: 44.8 months) as compared with those with TRPM1-low acral melanoma (median OS: undefined) (log-rank P = 0.0231 with a hazard ratio = 5.066, 95% confidence interval, 1.250–20.54; Fig. 1F). This finding suggests that the prognostic significance of TRPM1 protein level is associated with an early stage of acral melanoma.

Finally, we evaluated the association between the *TRPM1* mRNA expression and OS of patients with skin cutaneous melanoma using two public databases, OncoLnc and UALCAN. As shown in supplementary Fig. 1G, the analytic result from OncoLnc database showed that high *TRPM1* mRNA expression was closely associated with low OS time of patients with cutaneous melanoma (median OS in a TRPM1-high group 63.67 months vs. 122.8 months in a TRPM1-low group, log-rank P = 0.0004 with a hazard ratio = 2.013, 95% confidence interval, 1.370–2.958). The data from the UALCAN database also demonstrated that high expression of *TRPM1* mRNA

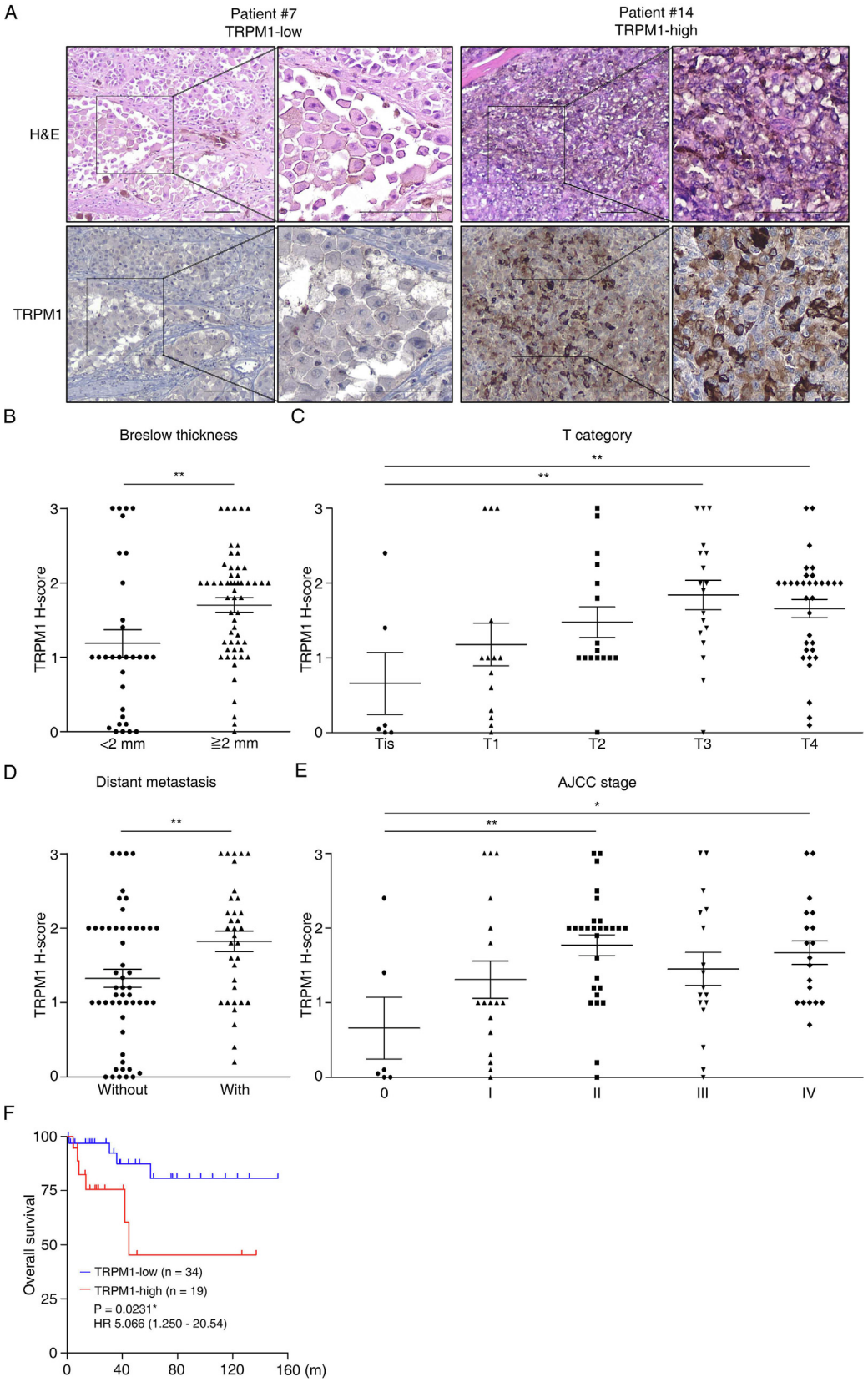

Fig. 1. TRPM1 was positively associated with tumor progression and poor survival in patients with acral melanoma. (**A**) Representative images of H&E staining and IHC analysis of TRPM1 expression in acral melanoma samples from patients. Magnified images of the boxed areas are shown. Scale bar: 100 μm. (**B**) TRPM1 expression versus the Breslow thickness of acral melanoma in the 87 patients. Breslow thickness < 2 mm, $n = 31$; Breslow thickness ≥ 2 mm, $n = 56$. (**C**) TRPM1 expression versus the T category of acral melanoma in the 87 patients. Tis, $n = 6$; T1, $n = 14$; T2, $n = 16$; T3, $n = 18$; T4, $n = 33$. (**D**) TRPM1 expression versus distant metastasis in the 87 patients. Patients with distal metastasis, $n = 53$; patients without distal metastasis, $n = 34$. (**E**) TRPM1 expression versus the AJCC stage in the 87 patients. Stage 0, $n = 6$; stage I, $n = 17$; stage II, $n = 28$; stage III, $n = 17$; stage IV, $n = 19$. The P values were determined by unpaired two-tailed Student's t-test, $^{*}P < 0.05$; $^{**}P < 0.01$. Data are mean ± SEM. (**F**) Kaplan-Meier survival curves of 53 patients without distant metastasis. Patients were separated into a TRPM1-high group (H-scores ≥ 2, $n = 19$, red curve) and a TRPM1-low group (H-score < 2, $n = 34$, blue curve). The P values were determined by the log-rank test.

was significantly associated with poor survival (P = 0.016). These results suggest that high *TRPM1* mRNA is positively associated with poor prognosis of patients with cutaneous melanoma.

Altogether, our results reveal that the level of TRPM1 expression is positively associated with tumor progression and could serve as a marker of poor prognosis in patients with acral melanoma.

TRPM1 activates AKT and promotes the growth, migration and invasion of melanoma cells and tumor growth

We investigated the role of TRPM1 in the tumor progression of melanoma cells. First, in cells in which TRPM1 was silencing, the levels of phospho-AKT were decreased. However, the levels of phospho-ERK were not decreased in TRPM1-silenced cells from either an acral melanoma cell line, MMG1, or a cutaneous melanoma cell line, Mel1617 (Fig. 2A and supplementary Fig. 2A). The silencing of TRPM1 suppressed clonogenic cell growth (Fig. 2B and supplementary Fig. 2B) and the subcutaneous xenograft tumor growth of MMG1 and Mel1617 cells (Fig. 2C and supplementary Fig. 2C–D). IHC assays revealed that levels of TRPM1, phospho-AKT and Ki67 (a marker for actively proliferating tumor cells) were decreased in tumors expressing TRPM1 shRNA#74 but not in tumors expressing scrambled shRNA (Fig. 2D). Next, we observed that the overexpression of 3xF-TRPM1 increased phospho-AKT levels but did not affect the levels of phospho-ERK in either MMG1 or Mel1617 cells (Fig. 2E and supplementary Fig. 2E). The ability to grow as colonies in clonogenic and anchorage-independent cell growth assays was better in MMG1 cells expressing 3xF-TRPM1 than in control cells (Fig. 2F and supplementary Fig. 2F). 3xF-TRPM1 expression also promoted MMG1 cell migration and invasion (Fig. 2G and supplementary Fig. 2G). Similar results were observed in Mel1617 cells (supplementary Fig. 2H–I). Compared to the empty-vector group, the group expressing 3xF-TRPM1 markedly promoted xenograft tumor growth (Fig. 2H and supplementary Fig. 2J–K). The tumors expressing 3xF-TRPM1 had higher levels of phospho-AKT and Ki67 (Fig. 2I). These tumor-bearing animals did not exhibit reduced body weight (supplementary Fig. 2L). Our findings suggest that TRPM1 promotes AKT signaling, cell migration and invasion, and xenograft tumor growth in melanoma cells.

TRPM1 promotes AKT activation through Ca^{2+}/calmodulin-dependent kinase IIδ

We then determined the molecular mechanisms by which TRPM1 promotes tumor growth. As TRPM1 is a Ca^{2+} channel, the levels of cytosolic Ca^{2+} were lower in cells expressing TRPM1 shRNAs than in cells expressing scrambled shRNAs (Fig. 3A) and higher cytosolic Ca^{2+} concentrations were detected in cells expressing 3xF-TRPM1 than in cells carrying the empty vector (Fig. 3B). Notably, the autophosphorylation levels of Ca^{2+}/calmodulin-dependent protein kinase II at Thr286/287 (P-CaMKII) were decreased upon TRPM1 knockdown but were increased in response to TRPM1 overexpression (Fig. 3A–B and supplementary Fig. 3A–B). These results show that TRPM1 regulates cytosolic Ca^{2+} concentrations and CaMKII activity in melanoma cells.

To determine which isoform of CaMKII plays a major role in mediating Ca^{2+} signaling in melanoma, qPCR was carried out to quantify the mRNA levels of *CaMKIIγ* and *CaMKIIδ*. These isoforms are expressed in various tissues, whereas α and β isoforms are predominantly present in neurons. We found that the levels of *CaMKIIδ* mRNA were higher than those of *CaMKIIγ* (supplementary Fig. 3C). Neither the knockdown nor overexpression of TRPM1 affected their expression levels (supplementary Fig. 3D). After confirming the knockdown efficiency and specificity of shRNAs against *CaMKIIγ* and *CaMKIIδ* using qPCR (supplementary Fig. 3E) and western blotting (supplementary Fig. 3F), we found that CaMKIIδ knockdown markedly decreased the levels of TRPM1-promoted AKT phosphorylation in MMG1 cells (Fig. 3C and supplementary Fig. 3G). These findings show that CaMKIIδ plays a crucial role in TRPM1 signaling. Next, we sought to examine whether TRPM1 promotes the CaMKIIδ/AKT interaction. Co-immunoprecipitation assays using lysates from MMG1 cells stably carrying the empty vector or expressing 3xF-TRPM1 were performed. Western blotting analysis indicated that CaMKIIδ coprecipitated with the anti-AKT antibody-conjugated agarose but not with the control IgG precipitates. Furthermore, this CaMKIIδ/AKT interaction was promoted by 3xF-TRPM1 (Fig. 3D and supplementary Fig. 3H).

To examine the requirement of phospho-CaMKIIδ at Thr287 for the association of CaMKIIδ/AKT, we generated a phosphomimetic CaMKIIδ mutant (F-CaMKIIδ-TD) in which the Thr287 residue was substituted with Asp, and a phospho-defective mutant (F-CaMKIIδ-TA) in which the Thr287 residue was replaced by Ala. As shown in Fig. 3E and supplementary Fig. 3I, the CaMKIIδ/AKT interaction was enhanced by the TD mutant of CaMKIIδ but it was abolished by the TA mutant. Consistently, the cells expressing F-CaMKIIδ-TD had increased levels of AKT phosphorylation, but these levels were decreased by CaMKIIδ-TA. These results suggest that the phosphorylation of CaMKIIδ at T287 is crucial for the CaMKIIδ/AKT interaction and AKT activation. Notably, the attenuation of AKT activity by TRPM1 knockdown was partially restored when cells expressed F-CaMKIIδ-TD. TRPM1-promoted AKT activation was enhanced in cells expressing wild-type CaMKIIδ but not F-CaMKIIδ-TA (Fig. 3F and supplementary Fig. 3J). Our investigation revealed a molecular mechanism by which TRPM1 promotes the CaMKIIδ/AKT interaction and AKT activation in melanoma.

The tumor-promoting activity of TRPM1 is mediated by CaMKIIδ.

We next examined whether CaMKIIδ mediates TRPM1-promoted cell growth, migration, and invasion. The results indicated that silencing *CaMKIIδ* inhibited the TRPM1-promoted proliferation (Fig. 3G), clonogenic growth, and anchorage-independent colony growth of MMG1 cells (Fig. 3H and supplementary Fig. 3K). *CaMKIIγ* knockdown did not inhibit the TRPM1-promoted proliferation (supplementary Fig. 3L). Additionally, cells expressing *CaMKIIδ* shRNAs markedly inhibited TRPM1-promoted cell migration and invasion (Fig. 3I and supplementary Fig. 3M). Moreover, gain-of-function experiments showed that CaMKIIδ-WT increased colony formation compared to the empty-vector control, suggesting that the elevated expression of CaMKIIδ is sufficient to promote colony growth. The expression of CaMKIIδ-TD did not further promote colony formation in MMG1 cells, and CaMKIIδ-TA inhibited colony formation (supplementary Fig. 3N). We observed that the expression of CaMKIIδ-TD partially rescued the inhibition of colony formation caused by TRPM1 knockdown, and CaMKIIδ-TA reduced the colonies promoted by 3xF-TRPM1 (Fig. 3J and supplementary Fig. 3O–P). Altogether, we demonstrated the role of phospho-CaMKIIδ at T287 in the mechanism underlying the tumor-promoting activity of TRPM1.

CaMKII inactivation reduces the tumor-promoting activity of TRPM1

We then sought to examine the possibility of suppressing melanoma growth by targeting CaMKIIδ using KN93. KN93 is a CaMKII pharmacological inhibitor that directly binds to Ca^{2+}/CaM and inactivates CaMKII [28]. The results showed that KN93 treatment decreased the levels of TRPM1-induced CaMKII and AKT phospho-

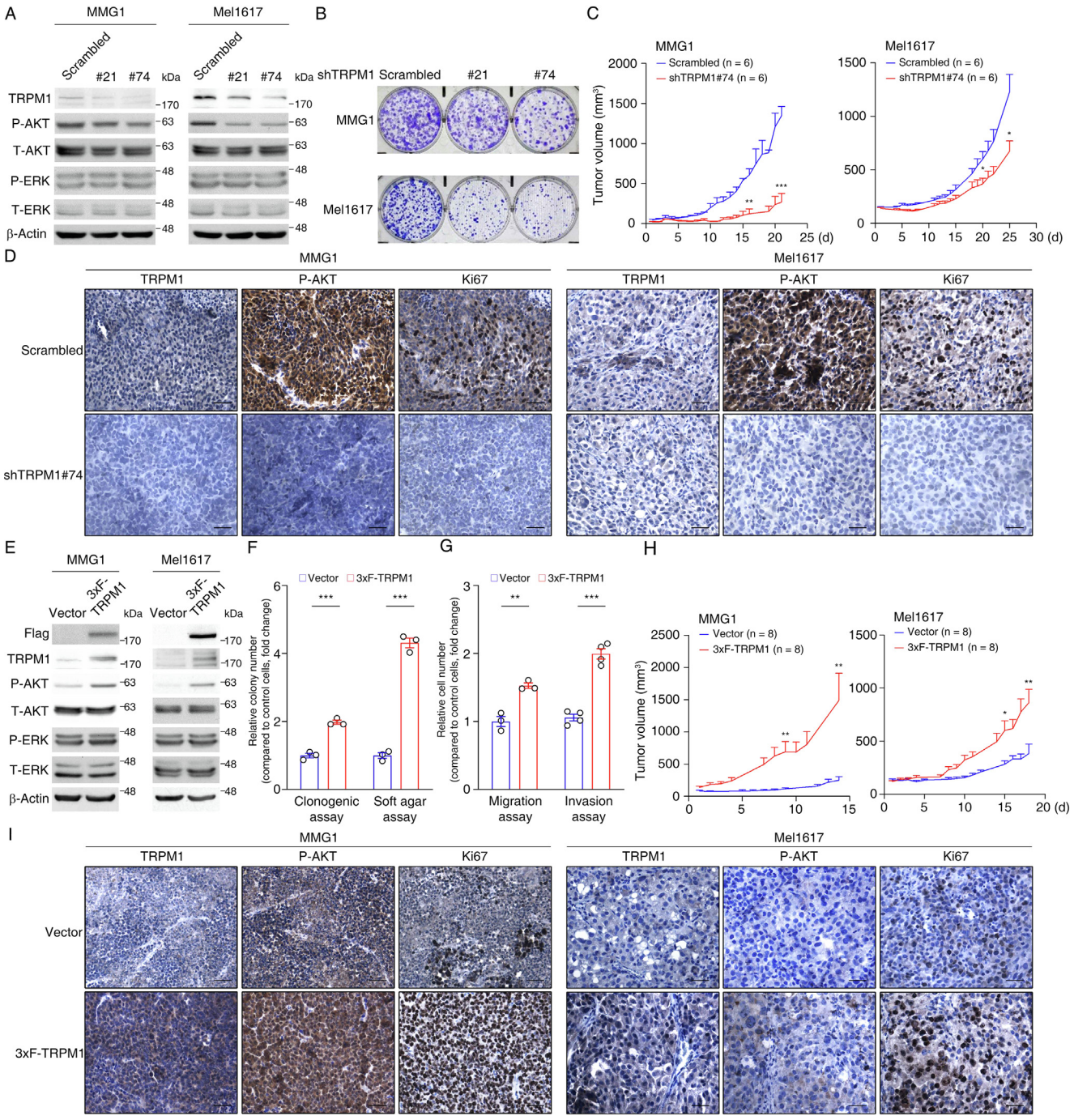

Fig. 2. TRPM1 activated AKT and promoted the growth, migration and invasion of melanoma cells and tumor growth. (**A**) Representative western blots of cells stably expressing either a scrambled shRNA or shRNAs specific for *TRPM1*. β -Actin served as a loading control, $n = 3$. (**B**) Representative images of clonogenic growth assays of cells stably expressing either a scrambled shRNA or *TRPM1* shRNAs, $n = 3$. (**C**) Quantification of tumor growth curves for the mice bearing xenograft tumors derived from cells stably expressing either a scrambled shRNA or *TRPM1* shRNA, $n = 6$. (**D**) Representative images of IHC analysis of TRPM1, phospho-AKT Thr308 (P-AKT) and Ki67 levels of xenograft tumor samples from the TRPM1 knockdown experiments, $n = 6$. (**E**) Representative western blots of cells stably carrying the empty vector or expressing 3xF-TRPM1, $n = 3$. (**F**) Quantification of clonogenic growth ($n = 3$), soft agar colony formation ($n = 3$), (**G**) cell migration ($n = 3$) and invasion ($n = 4$) assays in cells stably carrying the empty vector or expressing 3xF-TRPM1. (**H**) Quantification of tumor growth curves for the mice bearing xenograft tumors originating from cells stably carrying the empty vector or expressing 3xF-TRPM, $n = 8$. (**I**) Representative images of IHC analysis of TRPM1, P-AKT and Ki67 levels of xenograft tumor samples from the TRPM1 overexpression experiments, $n = 8$. Scale bar: 50 μm. The *P* values were determined by unpaired two-tailed Student's *t*-test, $^{*}P < 0.05$; $^{**}P < 0.01$; $^{***}P < 0.001$. Data are mean ± SEM.

rylation in a dose-dependent manner (Fig. 4A and supplementary Fig. 4A) and disrupted the TRPM1-promoted endogenous CaMKIIδ/AKT interaction (Fig. 4B and supplementary Fig. 4B). These findings suggest that KN93 blocks CaMKIIδ signaling by inhibiting CaMKII phosphorylation and interrupting the CaMKIIδ/AKT interaction to prevent TRPM1-promoted Ca^{2+}/CaMKIIδ/AKT axis activation.

Notably, we found that KN93 was toxic to MMG1 cells with a half-maximal inhibitory concentration (IC_{50}) of 5.22 ± 0.3 μM. However, KN93 did not reduce Mel1617 cell viability. TRPM1 expression did not influence the sensitivity to KN93 in either MMG1 or Mel1617 cells (supplementary Fig. 4C). This may be because (1) the short-term 72 h mitochondrial respiration activity-based assay could not detect the impact of KN93 on cell

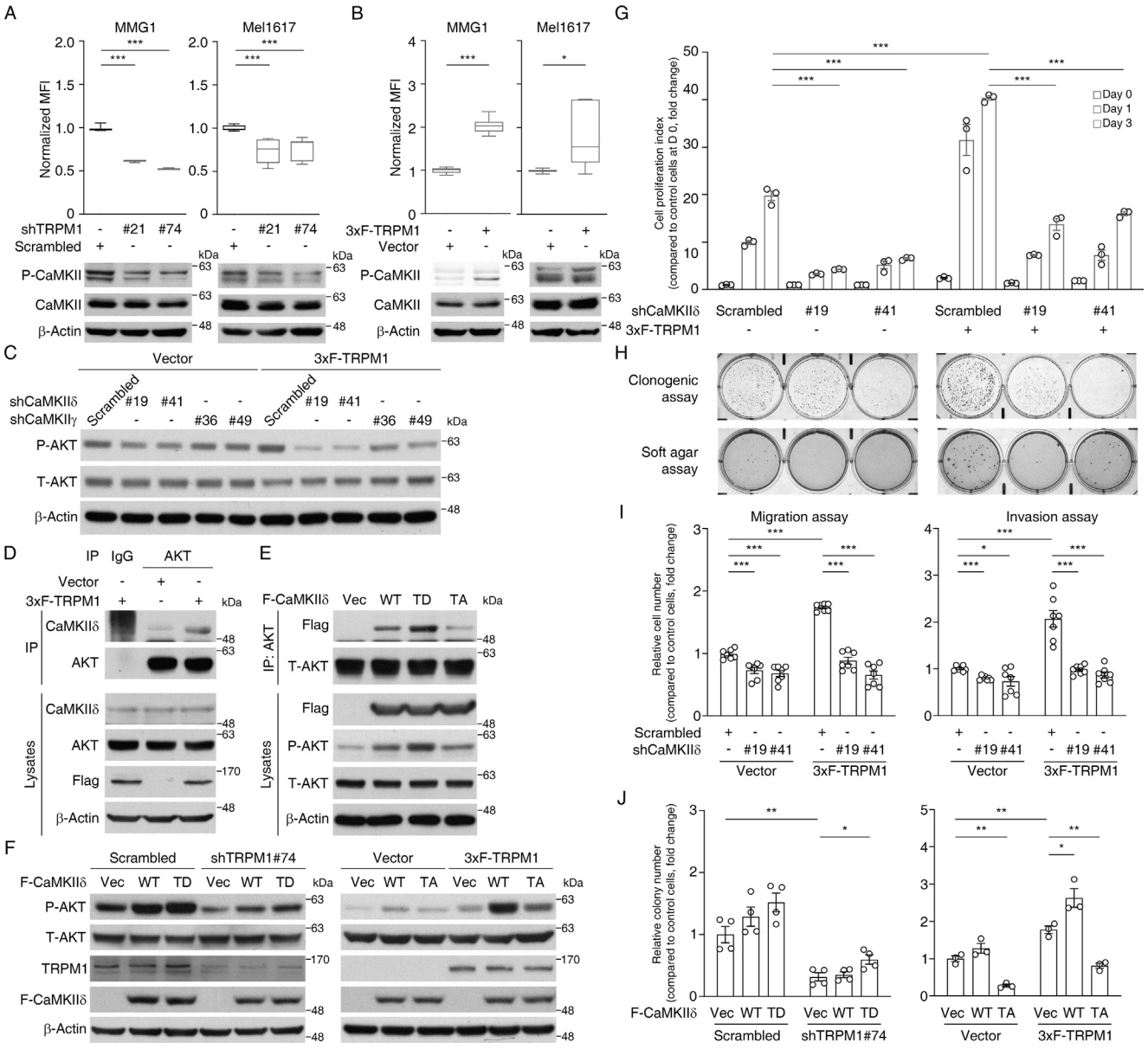

Fig. 3. TRPM1 promoted cell growth and mobility by activating the Ca^{2+}/CaMKIIδ/AKT pathway. (**A**) Quantification of cytosolic Ca^{2+} levels (upper) and representative western blots (bottom) in cells stably expressing either a scrambled shRNA or *TRPM1* shRNAs ($n = 3$), or (**B**) in cells stably carrying the empty vector or expressing 3xF-TRPM1 ($n = 3$). (**C**) Representative western blots for CaMKIIδ or CaMKIIγ knockdown experiments on MMG1 cells stably carrying the empty vector or expressing 3xF-TRPM1, $n = 3$. (**D**) Representative western blots of CaMKIIδ coimmunoprecipitated with anti-AKT antibody-conjugated agarose in lysates from MMG1 cells stably carrying the empty vector or expressing 3XF-TRPM1. Mouse IgG antibodies served as an IP control, $n = 3$. (**E**) Representative western blots of F-CaMKIIδ coimmunoprecipitated with anti-AKT antibody-conjugated agarose in lysates from MMG1 cells stably carrying the empty vector or expressing F-CaMKIIδ constructs as indicated, $n = 3$. (**F**) Representative western blots of TRPM1 knockdown and 3xF-TRPM1 overexpression experiments on MMG1 cells stably carrying the empty vector or expressing F-CaMKIIδ constructs as indicated, $n = 3$. (**G**) Cell proliferation assays for CaMKIIδ knockdown experiments on MMG cells stably carrying the empty vector or expressing 3xF-TRPM1 at the indicated time points, $n = 3$. (**H**) Representative images of clonogenic growth and soft agar colony formation assays for CaMKIIδ knockdown experiments, $n = 3$. (**I**) Quantification of cell migration and invasion assays for CaMKIIδ knockdown experiments, $n = 7$. (**J**) Quantification of clonogenic growth for TRPM1 knockdown (left, $n = 4$) and 3xF-TRPM1 overexpression (right, $n = 3$) experiments on MMG1 cells stably carrying the empty vector or expressing F-CaMKIIδ constructs as indicated. *P* values were determined by unpaired two-tailed Student's *t*-test, $^{*}P < 0.05$; $^{**}P < 0.01$; $^{***}P < 0.001$. Data are mean ± SEM.

growth, or (2) the oncogenic BRAFV600E mutation could sustain the survival signaling, such as MAPK and AKT pathways and provide a huge growth advantage to the cancer cells by reducing the inhibitory effect of KN93. We then examined the effects of KN93 treatment using long-term colony formation assays and found that KN93 treatment inhibited TRPM1-promoted clonogenic growth (Fig. 4C and supplementary Fig. 4D) and anchorage-independent colony formation (Fig. 4D and supplementary Fig. 4E). Additionally, KN93 treatment also suppressed cell migration (Fig. 4E and supplementary Fig. 4F) and invasion (Fig. 4F and supplementary Fig. 4G). These findings suggested that KN93 inhibits the tumor-promoting activity of TRPM1 by disrupting the TRPM1-driven Ca^{2+}/CaMKIIδ/AKT pathway.

Pharmacological inhibition of CaMKII suppresses the growth of TRPM1-high acral melanoma.

Next, we sought to examine the association between the levels of P-CaMKII and TRPM1 in acral melanomas. We found that a significant upregulation of phospho-CaMKII levels in acral melano-

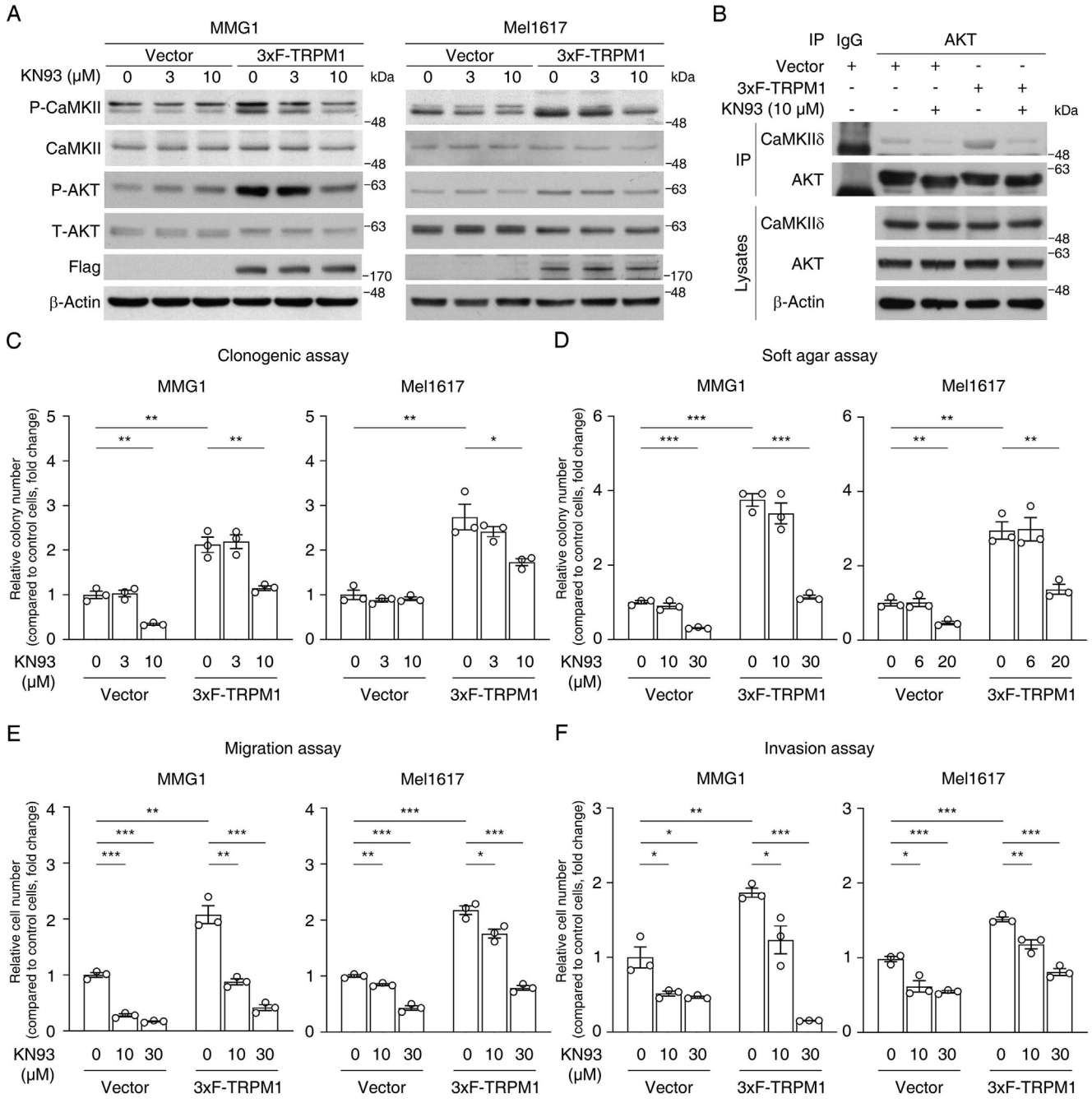

Fig. 4. CaMKII inactivation reduced the tumor-promoting activity of TRPM1. (**A**) Representative western blots of the KN93 treatment experiments on cells stably carrying the empty vector or expressing 3xF-TRPM1, $n = 3$. (**B**) Representative western blots of CaMKIIδ coimmunoprecipitated with anti-AKT antibody-conjugated agarose for the KN93 treatment experiments on MMG1 cells stably carrying the empty vector or expressing 3xF-TRPM1, $n = 3$. (**C**) Quantification of clonogenic growth, (**D**) soft agar colony formation, (**E**) migration, and (**F**) invasion assays for the KN93 treatment experiments on cells stably carrying the empty vector or expressing 3xF-TRPM1, $n = 3$. *P* values were determined by unpaired two-tailed Student's *t*-test, $^{*}P < 0.05$; $^{**}P < 0.01$; $^{***}P < 0.001$. Data are mean ± SEM.

mas was related to increased expression of TRPM1 by IHC analysis in a panel of FFPE specimens containing 14 TRPM1-high and 13 TRPM1-low acral melanomas from KMUH (Fig. 5A). TRPM1-high acral melanomas had higher P-CaMKII H-score than TRPM1-low acral melanomas (2.00 ± 0.1 vs. 1.27 ± 0.1, $P < 0.0001$; Fig. 5B and supplementary Fig. 5A). This result suggested that the increased P-CaMKII level is closely associated with high TRPM1 expression in acral melanomas.

The relevance of human cancer cell lines lies in their similarity to original tissues and their renewability. Their properties facilitate cancer research and the development of novel therapeutics. Several cutaneous melanoma cell lines have been established, but acral melanoma cell lines are difficult to establish. As shown in Fig. 4, KN93 treatment had modest effects on Mel1617 and MMG1 cell lines. These effects may result from a homozygous of BRAFV600E driver mutation in Mel1617 cells and a heterogeneity of the BRAFV600E mutation in MMG1 cells [29]. To avoid the complications resulting from BRAFV600E mutation, we established a primary acral melanoma cell line, CA11, with high TRPM1 expression and wild-type for BRAF and NRAS to evaluate the effects of KN93 on acral melanoma. CA11 cells were isolated from an acral melanoma with a TRPM1 H-score = 3.0 (supplementary Fig. 5B).

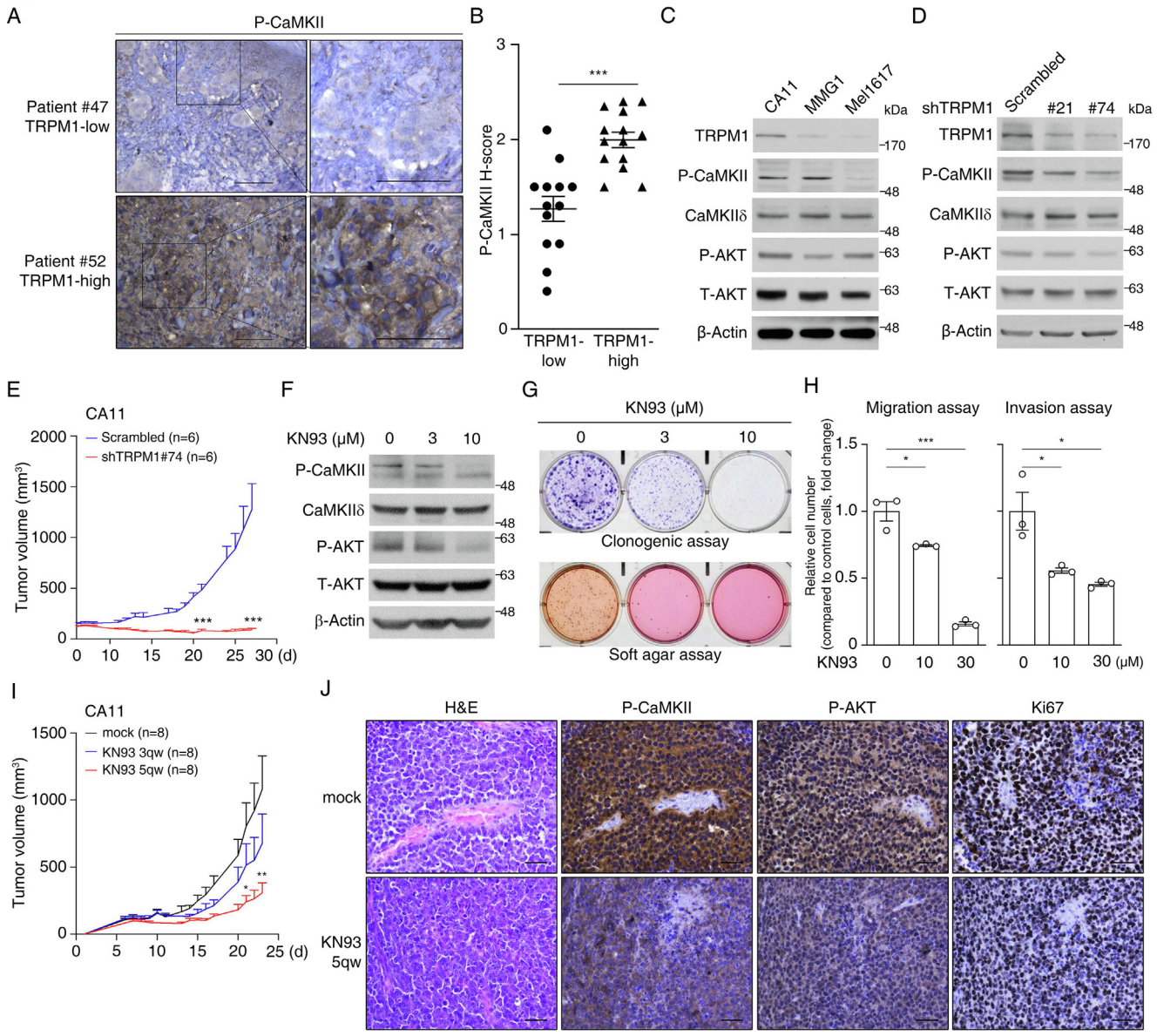

Fig. 5. KN93 suppressed the growth of TRPM1-high acral melanoma. (**A**) Representative images of IHC analysis of phospho-CaMKII (P-CaMKII) levels in acral melanoma samples from patients. Magnified images of the boxed areas are presented. Scale bar: 100 μm. (**B**) The H-score of P-CaMKII versus the TRPM1 expression in acral melanoma samples from 27 patients in the KMUH cohort. Patients were separated into a TRPM1-low group (H-score < 1.0, n = 13) and a TRPM1-high group (H-score greater than 2.0, n = 14). (**C**) Representative western blots of various human melanoma cells. (**D**) Representative western blots of CA11 cells expressing either a scrambled shRNA or *TRPM1* shRNAs, n = 3. (**E**) Quantification of tumor growth curves for the xenograft tumors originating from CA11 cells expressing either a scrambled shRNA or *TRPM1* shRNA, n = 6. (**F**) Representative western blots of the KN93 treatment experiments on CA11 cells, n = 3. (**G**) Representative images of clonogenic growth and soft agar colony formation assays for the KN93 treatment experiments on CA11 cells, n = 3. (**H**) Quantification of cell migration and invasion assays for the KN93 treatment experiments on CA11 cells, n = 3. (**I**) Quantification of tumor growth curves for the mice bearing CA11 xenograft tumors treated with a mock agent (n = 8), 10 mg/kg KN93 three times weekly (3qw, n = 8), or five times weekly (5qw, n = 8) by intraperitoneal injection. (**J**) Representative images of H&E staining and IHC analysis of P-CaMKII, P-AKT, and Ki67 levels in CA11 xenograft tumor samples from the KN93 treatment experiments, Scale bar: 50 μm, n = 8. P values were determined by unpaired two-tailed Student's t-test, $^{*}P < 0.05$; $^{**}P < 0.001$; $^{***}P < 0.001$. Data are mean ± SEM.

The mutation hotspots of BRAF at V600 and NRAS at G12/G13/Q61 were verified by Sanger sequencing to confirm the wild-type genotype of BRAF and NRAS (supplementary Fig. 5C). Western blotting showed that CA11 cells had a higher expression level of TRPM1 and increased phosphorylation of CaMKII and AKT compared to the other melanoma cell lines (Fig. 5C and supplementary Fig. 5D). The knockdown of TRPM1 decreased the phosphorylation levels of CaMKII and AKT (Fig. 5D and supplementary Fig. 5E) and reduced the xenograft tumor growth (Fig. 5E and supplementary Fig. 5F–G) of CA11 cells. Moreover, the treatment of KN93 reduced CaMKII and AKT activation (Fig. 5F and supplementary Fig. 5H), inhibited clonogenic and anchorage-independent cell growth (Fig. 5G and supplementary Fig. 5I), suppressed cell migration and invasion (Fig. 5H and supplementary Fig. 5J), and triggered cell apoptosis (supplementary Fig. 5K–L) of CA11 cells. Furthermore, MeWo cells are a cutaneous melanoma cell line featuring high expression of TRPM1 and are wild-type for BRAF and NRAS. These cells were also sensitive to KN93 treatment (supplementary Fig. 5M). These results suggest that melanomas with high expression of TRPM1 and wild-type for BRAF and NRAS that have elevated CaMKII signaling are sensitive to CaMKII inhibitor.

Finally, we evaluated the anti-tumor activity of KN93 using a subcutaneous xenograft model of CA11 human acral melanoma. The tumor-bearing mice were administered intraperitoneally

injections of either with a mock agent, KN93 at 10 mg/kg three times weekly (3qw), or KN93 at 10 mg/kg five times weekly (5qw) for 2 weeks. Mice treated with KN93 at either 3qw or 5qw showed a significant reduction in tumor growth compared to mock agent-treated animals during the 2 weeks of treatment (Fig. 5I and supplementary Fig. 5N–O). The body weights of the animals treated with KN93 were comparable to those of mock agent-treated animals (supplementary Fig. 5P). Tumors from mock agent- and KN93-treated tumor-bearing mice were collected and subjected to IHC analysis. We found that the administration of KN93 markedly reduced the phosphorylation levels of CaMKII and AKT and eliminated actively proliferating tumor cells (Fig. 5J). Our results strongly indicate that a therapeutic benefit may be achieved by means of a CaMKII inhibitor, such as KN93, in acral melanoma with TRPM1 overexpression.

Discussion

Clinically, we examined the relationship between the level of TRPM1 protein and the progression of acral melanoma. Tumors from 36 patients (41.4%) featured high TRPM1 protein levels. The prevalence of tumor thickness and distant metastasis was significantly increased among patients with acral melanomas with high expression of TRPM1. AJCC stages III and IV were significantly associated with TRPM1 protein levels. Patients with no distant metastasis and with high TRPM1 protein levels in the tumor presented significantly poorer OS. These results suggest that the expression of TRPM1 protein is positively associated with progression and may promote malignant transformation in acral melanoma. Mechanistically, we revealed that (1) TRPM1 elevates cytosolic Ca^{2+} levels to activate CaMKIIδ/AKT signaling. This could then lead to malignant transformation and the growth of tumor cells. (2) The Ca^{2+}/CaMKIIδ/AKT signaling is crucial for mediating the tumor-promoting activity of TRPM1 in melanoma cells. (3) The tumor-promoting activity of TRPM1 is suppressed by a CaMKII inhibitor, KN93. Our study suggests that CaMKII inhibition may be a potential therapeutic strategy for treating acral melanomas with high expression of TRPM1.

Three melanoma cell lines, MMG1 (acral melanoma with a heterogeneous BRAFV600E mutation), Mel1617 (cutaneous melanoma with a homozygous BRAFV600E mutation), and CA11 (acral melanoma with wild-type BRAF and NRAS) were employed to investigate the function of TRPM1. We found that CA11 cells were more sensitive to TRPM1 knockdown and KN93 treatment experiments than MMG1 and Mel1617 cells. Moreover, a cutaneous melanoma cell line, MeWo, that features high expression of TRPM1 and wild-type BRAF and NRAS was also sensitive to KN93 treatment. These observations support not only the tumor-promoting activity of TRPM1 in melanoma, but also our hypothesis that BRAFV600E melanomas may not require the TRPM1/CaMKIIδ/AKT pathway for their growth and malignancy and have modest effects in response to CaMKII inhibitor treatment. By contrast, melanomas with high expression of TRPM1 and wild-type for BRAF and NRAS have elevated CaMKII signaling are sensitive to CaMKII inhibitor.

Studies have suggested that TRPM1 is involved in synapse formation and to mediate the mGluR6 signaling to depolarize the light response in retinal ON-bipolar cells [30–32]. A recent study has also revealed that TRPM1 regulates the cytosolic Ca^{2+} concentration [33]. These findings indicate that TRPM1 regulates a variety of cellular functions by governing cytosolic Ca^{2+} levels. Ca^{2+}, a type of secondary messenger, allosterically activates enzymes and proteins that integrate signals from intrinsic and extrinsic stimulation to mediate diverse cellular processes in a cell type- and tissue context-dependent manner. Calmodulin (CaM), a Ca^{2+}-sensing protein, binds to and confers Ca^{2+}-sensitivity on enzymes, such as Ca^{2+}/CaM-dependent Ser/Thr protein kinase (CaMK). This transduces intracellular calcium signals by phosphorylating and activating a variety of downstream proteins to regulate multiple cellular functions [34,35]. CaMKII is a metastasis-promoting protein present in various cancer subtypes. CaMKIIα has been suggested to support tumor-initiating cells by activating EZH2/SOX2 signaling in lung cancer [36], to promote NF-kB- and AKT-mediated MMP-9 production to regulate gastric cancer cell metastasis [37], to increase the cell migration, invasiveness, and anchorage-independent growth of breast cancer cells [38], and to be associated with the proliferation and metastasis of colon cancer cells [39]. CaMKIIγ is highly activated together with β -Catenin and STAT3 signaling in leukemia stem cells [40] and may support tumor-initiating cells in an AKT- and β -Catenin-dependent manner in lung cancer [41]. Here, we found that CaMKIIδ is the predominant isoform of CaMKII expressed in melanoma cells. CaMKIIδ senses a TRPM1-induced Ca^{2+} surge to interact with AKT and activate AKT signaling, leading to the malignant transformation of melanoma cells.

The small molecule compound KN93, which allosterically inactivates CaMKII by binding to Ca^{2+}/CaM has been widely used as an inhibitor to study the functions of CaMKII [28]. Animal studies suggest that KN93 treatment may serve as a therapeutic strategy against autoimmune diseases [42,43], ischemic heart disease [44], and the xenograft tumor growth of osteosarcoma [45]. Nonetheless, the poor selectivity of KN93 elevates the risk of adverse effects and limits its clinical applications. KN93 is not a specific or potent inhibitor of CaMKII and exerts inhibitory effects on several Ca^{2+}-regulated kinases such as CaMKI, CaMKIV, Lck [46], and MLCK [47] and Ca^{2+}-permeable channels such as Cav1 [48] and InsP3Rs [49]. However, KN93 has good potential to suppress tumor-promoting pathways derived from dysregulated Ca^{2+} signaling.

Our studies revealed that TRPM1 protein levels strongly correlate with several clinicopathological factors of acral melanoma and may represent a prognostic marker of acral melanoma. The phosphorylation of CaMKIIδ at Thr287 mediates TRPM1-promoted AKT activation by inducing the CaMKIIδ/AKT interaction, leading to the malignant transformation of melanoma cells. We showed that KN93 inhibits the Ca^{2+}/CaMKIIδ/AKT pathway thereby suppressing malignancy and the xenograft tumor growth of acral melanoma cells with high expression of TRPM1. Therefore, targeting CaMKII is a potential therapeutic avenue for acral melanomas with high expression of TRPM1.

Conclusion

TRPM1 promotes tumor progression and malignant transformation via activating the Ca^{2+}/CaMKIIδ/AKT pathway in acral melanoma. CaMKII inhibition may be a potential therapeutic strategy for treating acral melanomas with high expression of TRPM1.

Materials and Methods

Patient samples, IHC analysis, and establishment of an acral melanoma cell line.

A total of 87 patients with acral lentiginous melanoma were recruited at two different sites: the KMUH (Kaohsiung, Taiwan, 44 patients) from 2008 to 2019 and the KUH (Fukuoka, Japan, 43 patients) from 2001 to 2012. All patients provided signed informed consent prior to their inclusion in the study.

FFPE tumor biopsies were analyzed via H&E staining to confirm that a viable tumor was present. For IHC analysis, 4-μm-thick sections were prepared and subjected to 20% H_2O_2 treatment for 15–

18 h at room temperature to remove melanin before immersion in antigen unmasking buffer pH 9.0 (Vector Laboratories) for antigen retrieval. The sections were subjected with 3% H_2O_2 to eliminate endogenous peroxidase activity and blocked with PBS containing 5% of FBS and 0.5% of Triton X-100 before manual staining with primary antibodies: anti-TRPM1 (1:100, Santa Cruz) and anti-phospho-CaMKII β /γ/δ (pThr287) (1:500, Sigma-Aldrich), followed by incubation with the Dako Real Envision HRP/DAB detection reagent (Dako) according to the manufacturer's instructions. All sections were counterstained with hematoxylin (Muto Pure Chemicals) and mounted with the Malinol medium (Muto Pure Chemicals). The stained tissues were photographed using a light microscope (the gain was set to 1.0x, saturation to 1.00, and gamma to 1.01, Leica DM2000), and their histopathological characteristics were interpreted by two independent investigators. The expression of TRPM1 and P-CaMKII was semiquantitatively evaluated using the H-score [50]. The staining intensity was classified into no staining (0), weakly positive (1), moderately positive (2) and strongly positive (3). The H-score was calculated by multiplying the percentage of stained cells (0.00 to 1.00) by staining intensity ranging from 0 to 3, resulting in scores from 0 to 3.00.

To obtain primary-tumor material for cell culture, a tumor part approximately 0.5 cm^3 in size was excised from a surgical specimen of the macular part of a melanoma that developed on the sole of a 75-year-old Taiwanese woman who underwent surgical operations at KMUH in 2020. The sample was washed with ice-cold PBS containing 100 U/ml of penicillin–streptomycin (Gibco) and mechanically divided into 2–3 mm pieces, followed by enzymatic digestion with dispase II (Gibco) overnight at 4 °C. After a wash and resuspension in ice-cold PBS, the samples were filtered through a 70 mm nylon mesh. Cells were pelleted and resuspended in DMEM (HyClone) containing 10% of fetal bovine serum (FBS; Hyclone) with 100 U/ml of penicillin–streptomycin (Gibco) and seeded in a well of a 6-well plate. The medium was refreshed twice a week. The cell colonies were collected for further experiments.

Cell culture, transfection, and retroviral and lentiviral infection

293, A375, Mel1617, SK-MEL-28, 451-LU and MeWo cells were obtained from Dr. Bin Zheng. MMG1 cells were from Dr. Takamichi Ito. CA11 cells were derived from a primary specimen in this study. A375, SK-MEL-28, 451-LU and MeWo cells were cultured in RPMI1640 (HyClone); 293, Mel1617, MMG1, and CA11 cells were maintained in DMEM (HyClone) containing 10% fetal bovine serum (FBS; Hyclone) and 100 U/ml penicillin/streptomycin (Gibco). All cell lines tested negatively for mycoplasma with the MycoSensor PCR Assay Kit (Agilent Technologies).

For transfection, retroviral and lentiviral infection, the procedures were performed as previously described [33]. Briefly, 293 cells were polyethylenimine (PEI)-based transfected with Ampho packaging vector and pBabe-Puro retroviral vector encoding the gene of interest to produce retroviruses, or with packaging plasmids encoding VSV-G, gag-pol, rev, and pLKO or pLEX304 lentiviral vector encoding the gene of interest to produce to produce lentiviruses. The 48 h post-transfection of culture supernatants containing virus was collected and filtered by 0.45 μm filter, and infect cultured cells in the presence of 4 ug/ml polybrene (Sigma-Aldrich). When indicated, stable populations were obtained and maintained by selection with puromycin (Sigma-Aldrich) or blasticidin (InvivoGen).

For stably expressing a scrambled shRNA or shRNAs specific for *CaMKIIδ* in TRPM1-overexpressing MMG1 cells, an empty vector pLEX304 or pLEX304 carrying 3xF-TRPM1 was delivered to MMG1 cells by lentiviral infection and selected by blasticidin to generated TRPM1-overexpressing MMG1 cells, followed by CaMKIIδ knockdown, selected by blasticidin and puromycin selection. For stable knockdown of TRPM1 in CaMKIIδ-overexpressing MMG1 cells, either a scrambled shRNA or a shRNA specific for *TRPM1* was delivered to MMG1 cells stably carrying an empty vector or expressing F-CaMKIIδ constructs by lentiviral infection, followed by blasticidin and puromycin selection.

In vivo xenograft tumor growth studies

Four- to six-week-old female NOD/SCID mice (NCKU, Tainan, Taiwan) were housed in a specific pathogen-free environment in the animal facility of NCKU. 6×10^6 MMG1, Mel1617 or CA11 cells were mixed with Matrigel (1:1, BD Biosciences) and subcutaneously inoculated into the flanks of the mice. For KN93 treatment, when the tumor size reached about 100 mm^3, mice were randomly assigned to 3 groups: mock agent, KN93 3qw, KN93 5qw by the Research Randomizer at https://www.randomizer.org. No statistical method was used to predetermine sample size. The animals were intraperitoneally injected sunflower oil (mock agent, $n = 8$) or KN93. KN93 (10 mg/kg) was dissolved in DMSO, diluted in sunflower oil, and injected three times per week (3qw, $n = 8$) or five times per week (5qw, $n = 8$). In all studies, the tumors were monitored every day and harvested as indicated. The tumor size was calculated as volume = [length × $(width)^2$] / 2. The mice were euthanized when the tumor size was reached to 1000 mm^3 or after KN93 treatment for 2 w. The investigators were not blinded to group allocation or outcome assessment. No animals were excluded in these experiments. Mouse tissue sections were analyzed as same as patient samples described above.

Statistics

Statistical analyses were performed using Prism 8 (GraphPad Software). The *in vitro* experiments were done in biological triplicate each time and independently repeated at least 3 times. Data are presented as the mean ± SEM and the number (n) of samples used was as indicated. Unpaired two-tailed Student's *t*-test was used to compare differences between the control and experimental groups. Chi-square test was used to compare differences between TRPM1 expression and clinical pathological parameters in Table 1. Kaplan-Meier curves and log-rank tests were used to estimate event-time distributions, and hazards models were fitted to obtain estimates of hazard ratios. For all statistical analyses, differences were labeled as *, $P < 0.05$; **, $P < 0.01$; *** $P < 0.001$; ****; n. s. = not significant. P values < 0.05 was considered statistically significant.

Ethics statement

All experiments involving patient samples were conducted according to the approved protocols by the institutional review board at the Kaohsiung Medical University Hospital, Taiwan (KMUHIRB-F(I)-20200001 and KMUHIRB-E(II)-20200019) and the Kyushu University Hospital, Japan (30–363). All patients gave signed informed consent. All experiments involving animals were conducted according to the ethical policies and procedures approved by the institutional animal care and usage committee of the National Health Research Institutes, Taiwan (NHRI-IACUC-108041).

CRediT authorship contribution statement

Chi-Che Hsieh: Data curation, Formal analysis, Validation, Investigation, Visualization, Methodology, Writing – original draft, Writing – review & editing. **Yue-Chiu Su:** Resources, Data curation,

Formal analysis, Validation, Investigation, Visualization, Methodology, Writing – review & editing. **Kuan-Ying Jiang:** Data curation, Formal analysis, Validation, Investigation, Visualization, Methodology. **Takamichi Ito:** Resources, Data curation, Formal analysis, Validation, Investigation, Visualization, Methodology. **Ting-Wei Li:** . **Yumiko Kaku-Ito:** Resources, Data curation, Formal analysis, Validation, Investigation, Visualization, Methodology. **Shih-Tsung Cheng:** Resources, Data curation, Funding acquisition. **Li-Tzong Chen:** Formal analysis, Funding acquisition. **Daw-Yang Hwang:** Resources. **Che-Hung Shen:** Conceptualization, Resources, Data curation, Formal analysis, Supervision, Funding acquisition, Validation, Investigation, Methodology, Writing – original draft, Project administration, Writing – review & editing.

Declaration of Competing Interest

The authors declare that they have no known competing financial interests or personal relationships that could have appeared to influence the work reported in this paper.

Acknowledgements

This study was supported in part by the National Health Research Institutes, Taiwan (CA-110-PP-23), the Kaohsiung Medical University, Taiwan (KMU-KI109003), and the Ministry of Science and Technology, Taiwan (MOST 107-2314-B-400-036-MY3). We thank the technical services provided by the Bio-image Core Facility of the National Core Facility Program for Biotechnology, Ministry of Science and Technology, Taiwan.

Availability of data and materials

The data and materials underlying this article are available upon reasonable request to chshen@nhri.edu.tw.

Appendix A. Supplementary data

Supplementary data to this article can be found online at https://doi.org/10.1016/j.jare.2022.03.005.

References

[1] Rabbie R, Ferguson P, Molina-Aguilar C, Adams DJ, Robles-Espinoza CD. Melanoma subtypes: genomic profiles, prognostic molecular markers and therapeutic possibilities. J Pathol 2019;247(5):539–51.
[2] Huang K, Fan Ji, Misra S. Acral Lentiginous Melanoma: Incidence and Survival in the United States, 2006–2015, an Analysis of the SEER Registry. J Surg Res 2020;251:329–39.
[3] Hayward NK, Wilmott JS, Waddell N, Johansson PA, Field MA, Nones K, et al. Whole-genome landscapes of major melanoma subtypes. Nature 2017;545 (7653):175–80.
[4] Smalley KSM. Understanding melanoma signaling networks as the basis for molecular targeted therapy. J Invest Dermatol 2010;130(1):28–37.
[5] Akbani R, Akdemir K, Aksoy BA, Albert M, Ally A, Amin S, et al. Genomic Classification of Cutaneous Melanoma. Cell 2015;161(7):1681–96.
[6] Wan PTC, Garnett MJ, Roe SM, Lee S, Niculescu-Duvaz D, Good VM, et al. Mechanism of activation of the RAF-ERK signaling pathway by oncogenic mutations of B-RAF. Cell 2004;116(6):855–67.
[7] Luke JJ, Flaherty KT, Ribas A, Long GV. Targeted agents and immunotherapies: optimizing outcomes in melanoma. Nat Rev Clin Oncol 2017;14(8):463–82.
[8] Ito T, Kaku-Ito Y, Murata M, Furue K, Shen C-H, Oda Y, et al. Immunohistochemical BRAF V600E Expression and Intratumor BRAF V600E Heterogeneity in Acral Melanoma: Implication in Melanoma-Specific Survival. J Clin Med 2020;9(3):690. doi: https://doi.org/10.3390/jcm9030690.
[9] Dika E, Veronesi G, Altimari A, Riefolo M, Ravaioli GM, Piraccini BM, et al. BRAF, KIT, and NRAS Mutations of Acral Melanoma in White Patients. Am J Clin Pathol. 2020;153(5):664-71.
[10] Newell F, Wilmott JS, Johansson PA, Nones K, Addala V, Mukhopadhyay P, et al. Whole-genome sequencing of acral melanoma reveals genomic complexity and diversity. Nat Commun 2020;11(1). doi: https://doi.org/10.1038/s41467-020-18988-3.
[11] Hunter JJ, Shao J, Smutko JS, Dussault BJ, Nagle DL, Woolf EA, et al. Chromosomal localization and genomic characterization of the mouse melastatin gene (Mlsn1). Genomics 1998;54(1):116–23.
[12] Miller AJ, Du J, Rowan S, Hershey CL, Widlund HR, Fisher DE. Transcriptional regulation of the melanoma prognostic marker melastatin (TRPM1) by MITF in melanocytes and melanoma. Cancer Res 2004;64(2):509–16.
[13] Deeds J, Cronin F, Duncan LM. Patterns of melastatin mRNA expression in melanocytic tumors. Hum Pathol 2000;31(11):1346–56.
[14] Guo H, Carlson JA, Slominski A. Role of TRPM in melanocytes and melanoma. Exp Dermatol 2012;21(9):650–4.
[15] Erickson LA, Letts GA, Shah SM, Shackelton JB, Duncan LM. TRPM1 (Melastatin-1/MLSN1) mRNA expression in Spitz nevi and nodular melanomas. Mod Pathol 2009;22(7):969–76.
[16] Levy C, Khaled M, Iliopoulos D, Janas MM, Schubert S, Pinner S, et al. Intronic miR-211 assumes the tumor suppressive function of its host gene in melanoma. Mol Cell 2010;40(5):841–9.
[17] Lunavat TR, Cheng L, Einarsdottir BO, Olofsson Bagge R, Veppil Muralidharan S, Sharples RA, et al. BRAF(V600) inhibition alters the microRNA cargo in the vesicular secretome of malignant melanoma cells. Proc Natl Acad Sci U S A 2017;114(29). doi: https://doi.org/10.1073/pnas.1705206114.
[18] Vogel C, Marcotte EM. Insights into the regulation of protein abundance from proteomic and transcriptomic analyses. Nat Rev Genet 2012;13 (4):227–32.
[19] Kosti I, Jain N, Aran D, Butte AJ, Sirota M. Cross-tissue Analysis of Gene and Protein Expression in Normal and Cancer Tissues. Sci Rep 2016;6:24799.
[20] Liu Y, Beyer A, Aebersold R. On the Dependency of Cellular Protein Levels on mRNA Abundance. Cell 2016;165(3):535–50.
[21] Jimenez I, Prado Y, Marchant F, Otero C, Eltit F, Cabello-Verrugio C, et al. TRPM Channels in Human Diseases. TRPM Channels in Human Diseases Cells 2020;9 (12):2604. doi: https://doi.org/10.3390/cells9122604.
[22] Xu X-Z, Moebius F, Gill DL, Montell C. Regulation of melastatin, a TRP-related protein, through interaction with a cytoplasmic isoform. PNAS 2001;98 (19):10692–7.
[23] Devi S, Kedlaya R, Maddodi N, Bhat KMR, Weber CS, Valdivia H, et al. Calcium homeostasis in human melanocytes: role of transient receptor potential melastatin 1 (TRPM1) and its regulation by ultraviolet light. Am J Physiol Cell Physiol 2009;297(3):C679–87.
[24] Cox JL, Lancaster T, Carlson CG. Changes in the motility of B16F10 melanoma cells induced by alterations in resting calcium influx. Melanoma Res 2002;12 (3):211–9.
[25] Hunter T, Schulman H. CaMKII structure–an elegant design. Cell 2005;123 (5):765–7.
[26] Chao L, Stratton M, Lee I-H, Rosenberg O, Levitz J, Mandell D, et al. A mechanism for tunable autoinhibition in the structure of a human Ca2 +/calmodulin- dependent kinase II holoenzyme. Cell 2011;146(5):732–45.
[27] Soderling TR, Chang B, Brickey D. Cellular signaling through multifunctional Ca2+/calmodulin-dependent protein kinase II. J Biol Chem 2001;276 (6):3719–22.
[28] Wong MH, Samal AB, Lee M, Vlach J, Novikov N, Niedziela-Majka A, et al. The KN-93 Molecule Inhibits Calcium/Calmodulin-Dependent Protein Kinase II (CaMKII) Activity by Binding to Ca(2+)/CaM. J Mol Biol 2019;431(7):1440–59.
[29] Lin J, Goto Y, Murata H, Sakaizawa K, Uchiyama A, Saida T, et al. Polyclonality of BRAF mutations in primary melanoma and the selection of mutant alleles during progression. Br J Cancer 2011;104(3):464–8.
[30] Koike C, Obara T, Uriu Y, Numata T, Sanuki R, Miyata K, et al. TRPM1 is a component of the retinal ON bipolar cell transduction channel in the mGluR6 cascade. Proc Natl Acad Sci U S A 2010;107(1):332–7.
[31] Kozuka T, Chaya T, Tamalu F, Shimada M, Fujimaki-Aoba K, Kuwahara R, et al. The TRPM1 Channel Is Required for Development of the Rod ON Bipolar Cell-AII Amacrine Cell Pathway in the Retinal Circuit. J Neurosci 2017;37 (41):9889–900.
[32] Morgans CW, Zhang J, Jeffrey BG, Nelson SM, Burke NS, Duvoisin RM, et al. TRPM1 is required for the depolarizing light response in retinal ON-bipolar cells. Proc Natl Acad Sci U S A 2009;106(45):19174–8.
[33] Shen C-H, Hsieh C-C, Jiang K-Y, Lin C-Y, Chiang N-J, Li T-W, et al. AUY922 induces retinal toxicity through attenuating TRPM1. J Biomed Sci 2021;28(1). doi: https://doi.org/10.1186/s12929-021-00751-5.
[34] Swulius MT, Waxham MN. Ca(2+)/calmodulin-dependent protein kinases. Cell Mol Life Sci 2008;65(17):2637–57.
[35] Bagur R, Hajnóczky G. Intracellular Ca(2+) Sensing: Its Role in Calcium Homeostasis and Signaling. Mol Cell 2017;66(6):780–8.
[36] Wang S-Q, Liu J, Qin J, Zhu Y, Tin V-C, Yam JWP, et al. CAMK2A supported tumor initiating cells of lung adenocarcinoma by upregulating SOX2 through EZH2 phosphorylation. Cell Death Dis 2020;11(6). doi: https://doi.org/10.1038/s41419-020-2553-6.
[37] Liu Z, Han G, Cao Y, Wang Y, Gong H. Calcium/calmodulindependent protein kinase II enhances metastasis of human gastric cancer by upregulating nuclear factorkappaB and Aktmediated matrix metalloproteinase9 production. Mol Med Rep 2014;10(5):2459–64.
[38] Chi M, Evans H, Gilchrist J, Mayhew J, Hoffman A, Pearsall EA, et al. Phosphorylation of calcium/calmodulin-stimulated protein kinase II at T286 enhances invasion and migration of human breast cancer cells. Sci Rep 2016;6 (1). doi: https://doi.org/10.1038/srep33132.
[39] Chen W, An P, Quan X-J, Zhang J, Zhou Z-Y, Zou L-P, et al. Ca(2+)/calmodulin-dependent protein kinase II regulates colon cancer proliferation and migration via ERK1/2 and p38 pathways. World J Gastroenterol 2017;23(33):6111–8.

[40] Gu Y, Chen T, Meng Z, Gan Y, Xu X, Lou G, et al. CaMKII gamma, a critical regulator of CML stem/progenitor cells, is a target of the natural product berbamine. Blood 2012;120(24):4829–39.
[41] Chai S, Xu X, Wang Y, Zhou Y, Zhang C, Yang Y, et al. Ca2+/calmodulin-dependent protein kinase IIgamma enhances stem-like traits and tumorigenicity of lung cancer cells. Oncotarget 2015;6(18):16069–83.
[42] Koga T, Hedrich CM, Mizui M, Yoshida N, Otomo K, Lieberman LA, et al. CaMK4-dependent activation of AKT/mTOR and CREM-alpha underlies autoimmunity-associated Th17 imbalance. J Clin Invest 2014;124(5):2234–45.
[43] Ichinose K, Juang Y-T, Crispín JC, Kis-Toth K, Tsokos GC. Suppression of autoimmunity and organ pathology in lupus-prone mice upon inhibition of calcium/calmodulin-dependent protein kinase type IV. Arthritis Rheum 2011;63(2):523–9.
[44] He Q, Cheng J, Wang Y. Chronic CaMKII inhibition reverses cardiac function and cardiac reserve in HF mice. Life Sci 2019;219:122–8.
[45] Yuan K, Chung LW, Siegal GP, Zayzafoon M. alpha-CaMKII controls the growth of human osteosarcoma by regulating cell cycle progression. Lab Invest 2007;87(9):938–50.
[46] Franklin RA, Atherfold PA, McCubrey JA. Calcium-induced ERK activation in human T lymphocytes occurs via p56(Lck) and CaM-kinase. Mol Immunol 2000;37(11):675–83.
[47] Raina H, Zacharia J, Li M, Wier WG. Activation by Ca2+/calmodulin of an exogenous myosin light chain kinase in mouse arteries. J Physiol 2009;587(Pt 11):2599–612.
[48] Anderson ME, Braun AP, Wu Y, Lu T, Wu Y, Schulman H, et al. KN-93, an inhibitor of multifunctional Ca++/calmodulin-dependent protein kinase, decreases early afterdepolarizations in rabbit heart. J Pharmacol Exp Ther 1998;287(3):996–1006.
[49] Smyth JT, Abbott AL, Lee B, Sienaert I, Kasri NN, De Smedt H, et al. Inhibition of the inositol trisphosphate receptor of mouse eggs and A7r5 cells by KN-93 via a mechanism unrelated to Ca2+/calmodulin-dependent protein kinase II antagonism. The Journal of biological chemistry 2002;277(38):35061–70.
[50] Tanaka Y, Murata M, Shen C-H, Furue M, Ito T. NECTIN4: A Novel Therapeutic Target for Melanoma. Int J Mol Sci 2021;22(2):976. doi: https://doi.org/10.3390/ijms22020976.